Structural design of the reinforced concrete encasing the spiral case steel liner in hydropower powerhouses.

João Pedro Nunes Rosado

Instituto Superior Técnico, Portugal

May 2019

ABSTRACT

The spiral case is a fundamental piece in the operation and energy generation of hydropower powerhouses. For the structural design of the reinforced concrete encasing the spiral case steel liner the most relevant actions are hydraulic actions that create internal pressures, with dynamic characteristics, inducing important solicitations on the surrounding structures. Particularly important for the design is to obtain the distribution of tensile forces between the liner and the encasing reinforced concrete according to the structural stiffness. Another aspect to consider is the complex geometry, which requires special care while implementing the numerical model on how it will behave. The scope of this current work is to elaborate a comparative study of the different methods of structural design of the spiral case encasing reinforced concrete, as well as to present the correspondent reinforced concrete detail design project, according to the given structural geometry.

KEYWORDS: Hydropower powerhouse; Reinforced concrete; Modelling; Hydrostatic pressure.

1. INTRODUTION

The spiral case is a fundamental piece in the operation and energy generation of hydropower powerhouses.

For the structural design of the reinforced concrete encasing the spiral case steel liner the most relevant actions are hydraulic actions that create internal pressures.

Particularly important for the design is to obtain the distribution of tensile forces between the liner and the encasing reinforced concrete according to the structural stiffness.

Another aspect to consider is the complex geometry, which requires special care while implementing the numerical model on how it will behave.

The scope of this current work is to elaborate a comparative study of the different methods of structural design of the spiral case encasing reinforced concrete, as well as to present the correspondent reinforced concrete detail design project, according to the given structural geometry from [3] (Figure 1.1 and Figure 1.2**Error! Reference source not found.**).

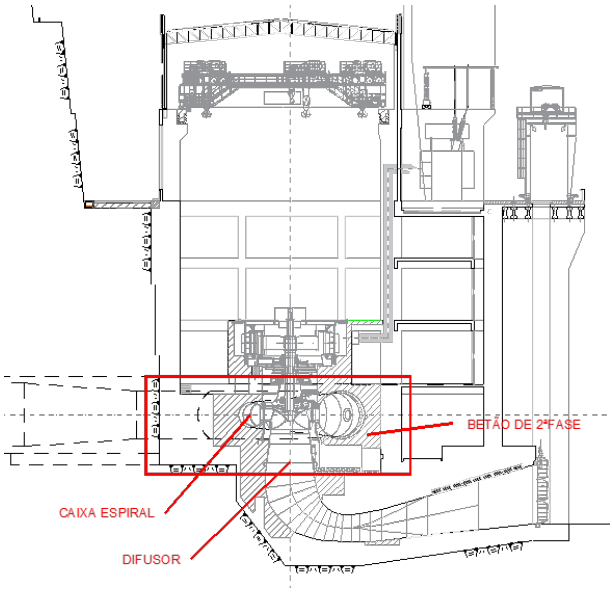

Figure 1.1: U/S-D/S vertical section through the turbine axis with identification of main parts (adapted from [3])

Figure 1.2: Example of reinforcement assembling surrounding spiral case for later concreting [10]

2. SPIRAL CASE GEOMETRY

Geometry of the case study, presented in Figure 2.1**Error! Reference source not found.**, corresponds to a Francis turbine with vertical axis, from [3]. Equally important to know are the geometries of the draft tube and the geometry of the generator shaft, as both parts are attached to the spiral case and therefore also embedded in the concrete that encases the spiral case.

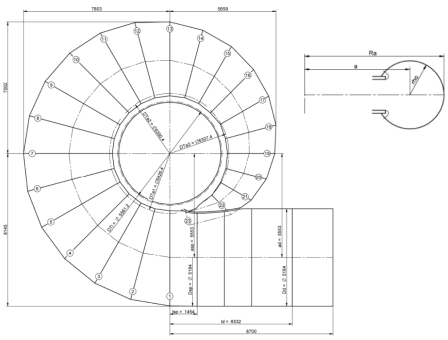

Figure 2.1: Plan view and typical cross section of case study spiral case [3].

The simplified geometry for the numerical model was created from a parallelepiped to which the volumes the voids of the spiral case, draft tube and generator shaft were subtracted.

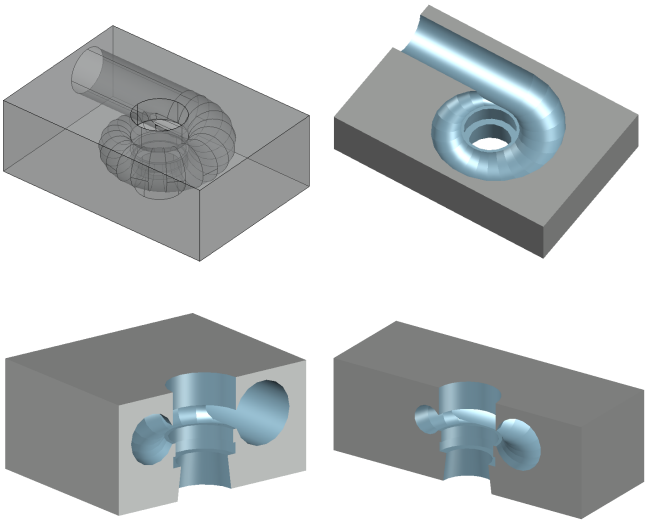

Figure 2.2: Different perspectives of the three-dimensional volume of the concrete encasing the spiral case.

2.1. Key sections for results comparison

To be able to compare the results from the different calculation methods, the key sections presented in Figure 2.3 were defined. These correspond to two vertical plane sections transversal to the spiral case axis and a horizontal plane section through the spiral case axis.

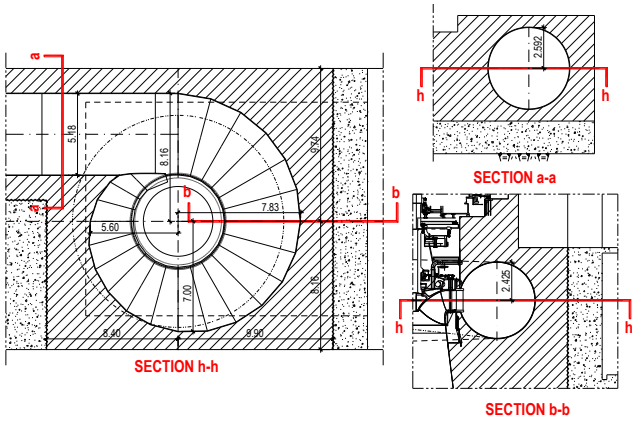

Figure 2.3: Key sections for results comparison.

3. MATERIALS, LOADS AND LOAD COMBINATIONS

3.1. Materials

The case study spiral case encasing concrete (2nd stage concrete) adopts the same concrete class as the 1st stage concrete, C30/37 as defined in [3].

This second stage concrete is, usually, a self-compacting concrete with small maximum aggregate size, to be able to efficiently cover the reinforcement bars. It must be noted that the concreting sequence can't be done too fast to avoid/limit the uplifting forces, but it can't be done too slow to avoid the formation of cold joints. Therefore, the usual procedure consists in performing a continuous concreting with layers of 0.30m to 0.60m thick, waiting for the concrete to start setting to begin the next layer.

Following [3], the reinforcement steel adopted was A500NR.

3.2. Loads

The loads considered for the design were:

- self-weight (concrete γ_c = 24 kN/m^3; Steel liner 30mm thick and γ_s = 78 kN/m^3);
- Super-imposed dead loads (total generator weight, Rotor + Stator, equal to 400t [3], considered as an equivalent uniform distributed load $F_{RCP,equiv} \cong 45\ kN/m^2$ according to Figure 3.1);
- Surcharges (weight of electromechanical equipment on floor above spiral case and service load, SC=15 KN/m^2 [3]);
- Hydrostatic pressure, (NPA = NMC = 130,0 m; EL turbine axis = 7,24 m, $P_{w,s} = 1228\ kN/m^2$)
- Hydrodynamic pressure, (Water hammer $P_{w,d,Hammer} = 1775\ kN/m^2$)

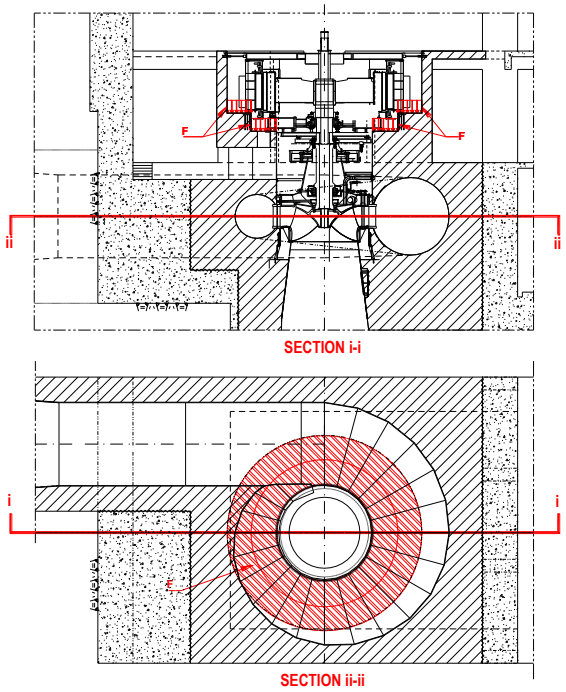

Figure 3.1: Generator weight equivalent load.

3.3. Loading conditions and Limit states verification

Water pressure inside the spiral case is the most pertinent load when compared to the remaining loads.

As water hammer load occurs frequently enough to be considered as a Normal Operation Condition, the critical load condition that was analysed was the one with the water hammer hydrodynamic pressure.

For the Ultimate Limit States verification, EN 1990 [6] criteria were followed, using unfavourable /favourable partial load factors. For water hammer load, a less conservative partial load factor was used, being followed instead the value proposed SIA 261 §4.4.3.4 Table 1 [8], as this water pressure is already the maximum water loads physically possible to have.

Therefore, the ULS combination considered was:

Combination	Load			
	SW	$F_{RCP,equiv}$	SC	$P_{w,d,Hammer}$
ULS	1,0	1,00	-	1,20

For the Service Limit States USACE EM 1110-2-2104 (3.7) [12] was used to control indirectly the crack opening and capacity to absorb vibrations in the encasing spiral case concrete. This is achieved by applying the Hydraulic factor, $H_f = 1{,}65$, to the ULS combination or equivalently by reducing the reinforcement yield stress.

4. METHODOLOGIES TO CONTROL HOW STRESSES ARE SHARED BETWEEN THE STEEL LINER AND THE ENCASING REINFORCED CONCRETE

Due to the high water pressures inside the spiral case, it is necessary to define how these should be resisted, taking in consideration the interaction between the steel liner and the encasing reinforced concrete in order to design a solution that is physically possible to build and also complies with the always constraining economic criteria.

According to [4], four main methodologies are defined.

Methodology 1 proposes the use of a compressible coating between the spiral case and the encasing concrete. When water pressures make the steel liner expand this coating compresses and no stress is transmitted to the surrounding concrete. This method has the disadvantage of requiring that the coating application is perfectly done which can have high execution costs.

Methodology 2 proposes to use the steel liner just as formwork, thus only atmospheric pressure inside the spiral case during concreting. Consequentially, as soon as the internal pressure rises, all the load is transmitted to the encasing concrete. This carries big consequences to the required amount of reinforcement needed that could easily become impossible to executable and un-economical.

Methodology 3 proposes to keep the steel liner at the maximum design internal pressure during concreting, so that the steel liner expands to the maximum design deflection. Consequentially, as soon as that the internal pressure reduces, a gap between the encasing concrete and the steel liner is created. This results that all internal pressures are resisted by the steel liner only, leaving the encasing concrete undisturbed. This method has the disadvantage of requiring higher efforts to maintain the internal pressure at maximum value for all the duration of the concreting operation. Furthermore, it forces that the generator loads are later mainly conveyed to the foundation through the stay ring, not taking advantage of the spiral case.

Methodology 4 proposes to keep the steel liner at a percentage (between 50% to 70%) of the Normal Operation Condition internal pressure during concreting, so that the steel liner suffers some expansion to create a future gap between the encasing concrete and the steel liner. This methodology assures that the steel liner is resisting all pressures below % $P_{NOC,}$ only transmitting the remaining pressures above this value to the encasing concrete.

Conclusions – Methodology 4 is the mostly used as it:

- Makes use of the steel liner stiffness to withstand the internal pressures;
- Reduces que pressure forces that are transmitted to the encasing concrete, thus reducing the amount of necessary reinforcement;
- Assures that the steel liner is in contact with the concrete during normal operation of the turbine. This is highly recommended to dampening the vibrations and allowing a better distribution of the loads from the generator.

Therefore, the maximum pressure that the steel liner can transmit to the encasing concrete is given by:

$$\Delta P_{w,d,Hammer} = P_{w,d,Hammer} - \% \times P_{NOC} \quad (1)$$

Nevertheless, above $\% \times P_{NOC}$, the interaction between the steel liner stiffness and the encasing concrete stiffness plays an additional role, allowing that part of the loads remains on the steel liner.

Quantifying how much is shared between the two materials is a complex process, and in the following chapters some methods are proposed.

For the current case study, considering that 70% of P_{NOC} stays in the steel liner, the maximum load transmitted to the encasing concrete is $\Delta P_{w,d,Hammer} = 947\ kN/m^2$.

5. TWO-DIMENSIONAL MODELLING

The two-dimensional modelling can be done either by simplified calculation using theoretical formulations, or by using plane finite elements modelling.

The theoretical formulations allow to better understand how the stresses are being resisted within the encasing concrete but require simple geometry to be applied. Therefore, when applying these formulations to the spiral case the results won't give accurate results.

The use of plane finite elements allows to study the correct geometry changes but can also produce results that aren't clear due inconsistencies in the mesh or boundary conditions incorrectly defined. Therefore, the designer experience plays an important role to detect these problems and calibrate correctly the model.

When combining these two approaches it is possible to obtain more results with higher degree of certainty.

5.1. Simplified calculation using theoretical formulations

To conceptualize the problem, two theoretical formulations were considered.

Formulation 1 – Hydrostatic pressure above % P_{NOC} is totally transferred to the encasing concrete – Reinforcement ring

This formulation follows a conservative approach considering that the spiral case stops resisting to internal pressure above % P_{NOC} transferring all additional pressure to the encasing concrete.

In reality, the electromechanical manufacturer designs the steel liner to withstand the full maximum internal design pressure on its own, therefore the steel liner still has capacity to continue to resist to the additional pressures above % P_{NOC} together with the encasing concrete.

For the encasing concrete, this formulation assumes that this is cracked, thus the concrete ring stiffness comes only from the ring reinforcement, ignoring the longitudinal reinforcement.

This behaviour is more easily understood if we imagine the three-dimensional surface of the spiral case developed into a flat "slab". In this view, it is clearly visible that the shortest "span" is the transversal (perpendicular to the spiral case axis) and therefore the slab is functioning as a one-way slab.

Consequentially, to considerer that the internal pressure will be resisted just by the ring reinforcement, $A_{s,cir}$, is a plausible simplification that guarantees equilibrium. This reinforcement is obtained by:

$$F = \Delta P_{int} \times r_{s,int} \quad ; \quad A_{s,cir} = \frac{F}{f_{yd}} \qquad (2)\ ;\ (3)$$

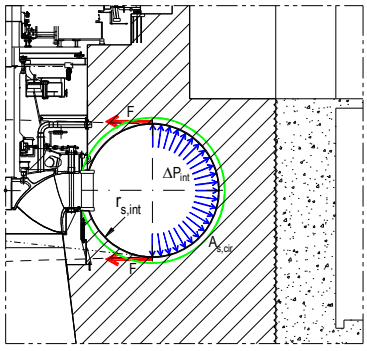

Figure 5.1:Tension force in the ring reinforcement

Formulation 2 – Hydrostatic pressure above % P_{NOC} is shared between the spiral case and the encasing concrete – Thick wall pipe theory – Lamé equations

As the spiral case steel liner is designed to resist the maximum hydrostatic pressure, it has the capacity to resist the expansion under the action of the additional hydrostatic pressures above % P_{NOC}, thus transferring less load to the encasing concrete as Formulation 1. On the other hand, when the steel liner expands it encounters the resistance from the encasing concrete, so the actual deformation will result from the consideration of the difference of magnitude of the steel and concrete modulus of elasticity.

To calculate the distribution of stresses between the steel and the concrete, Lamé equations applied to the theory of thick wall pipes for cylinders of composite sections can be used as a simplification of the problem.

The first step is to determine the pressure, p_c, at the contact surface between the steel liner and the concrete, by taking in consideration the relation between the modulus of elasticity of the two materials.

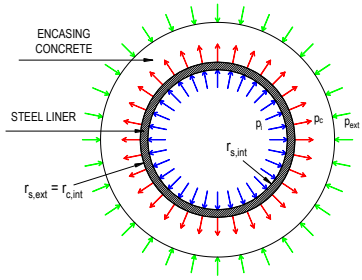

Figure 5.2: Identification of the pressures on the different surfaces.

$$p_c = p_i \frac{n \times k_s'}{n(k_s' + b_s) + (k_c' + 2 - b_c)} \qquad (4)$$

With:

$$p_i = \Delta P_{int}\ ; n = \frac{E_s}{E_c};\ b_s = 1 - \upsilon_s;\ b_c = 1 - \upsilon_c;$$

$$k_s' = \frac{2}{2 \times k_s + k_s^2} \quad ; \quad k_s = \frac{1}{r_{s,int}}\left(r_{s,ext} - r_{s,int}\right) \qquad (5)\ ;\ (6)$$

$$k_c' = \frac{2}{2 \times k_c + k_c^2} \quad ; \quad k_c = \frac{1}{r_{c,int}}\left(r_{c,ext} - r_{c,int}\right) \qquad (7)\ ;\ (8)$$

After knowing the value of the pressure p_c applied to the concrete, then it is possible to analyse the concrete ring using Lamé equations to determine the tangential stresses in the internal and external faces.

Considering that concrete can't resist to tension stresses, then the diagram of stresses along the cross section of the concrete ring is integrated to obtain the equivalent tension forces that will be considered to design the reinforcement areas.

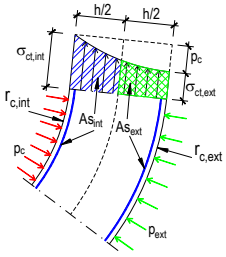

Figure 5.3: Tension stresses diagram along the transversal section of the encasing concrete ring.

$$\sigma_{t,int} = (p_c - p_{ext}) \times (1 + k'_c) - p_{ext} \quad (9)$$

if $p_{ext} = 0 \Rightarrow \sigma_{t,int} = p_c \times (1 + k'_c)$

$$\sigma_{t,ext} = (p_c - p_{ext}) \times k'_c - p_{ext} \quad (10)$$

if $p_{ext} = 0 \Rightarrow \sigma_{t,ext} = p_c \times k'_c$

$$r_{cm} = r_{c,int} + \frac{h}{2} \quad (11)$$

$$\sigma_{t,cm} = (p_c - p_{ext}) \times \left(\frac{r_{c,ext}^2}{r_{c,ext}^2 - r_{c,int}^2}\right) \times \left(\frac{r_{cm}^2 + r_{c,int}^2}{r_{cm}^2}\right) - p_c \quad (12)$$

if $p_{ext} = 0 \Rightarrow \sigma_{t,cm} = p_c \times \left(\frac{r_{c,ext}^2}{r_{c,ext}^2 - r_{c,int}^2}\right) \times \left(\frac{r_{cm}^2 + r_{c,int}^2}{r_{cm}^2}\right) - p_c$

And reinforcement calculation results from the integration of the stresses:

$$As_{int} = \int_{r_{c,int}}^{r_{cm}} \sigma_t \quad ; \quad As_{ext} = \int_{r_{cm}}^{r_{c,ext}} \sigma_t \quad (13) ; (14)$$

5.2. Plane finite element modelling calculation

The FEM allows to study different spiral case vertical cross sections considering the correct geometry. This will allow to obtain the expected ring tension stress but will provide also further information of zones where stress concentration exists, for example close to the stay ring.

Additionally, it is also possible to study the horizontal section through the spiral case axis to get an estimate of the longitudinal reinforcement.

Essential, is to properly define the boundary conditions to replicate the restrictions provided by the other parts of the powerhouse structure and adjacent monoliths.

The following figures exemplify these particularities of the boundary condition definition.

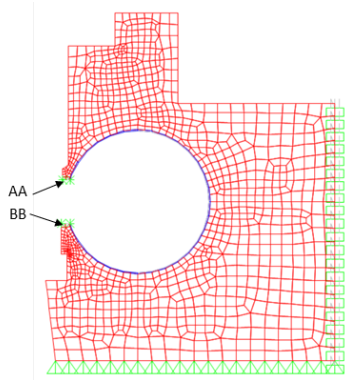

Figure 5.4: Section b-b, FEM mesh and supports.

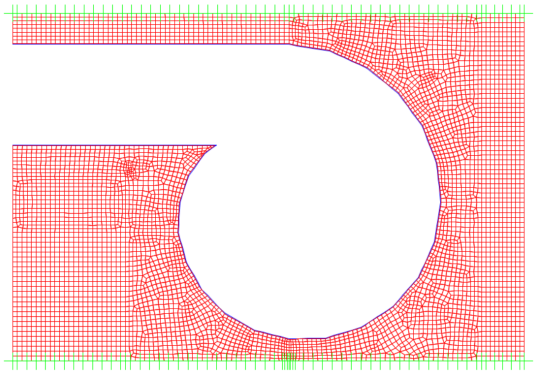

Figure 5.5: Section h-h, FEM mesh ans supports.

Contrary to the simplified formulations, the loads application using the 2D FEM allows to finally consider all the loads that are present at the same time, such as self-weight or generator loads and even how the internal pressure varies according to the geometry of the spiral case.

The following figures exemplify these particularities of the loads' application.

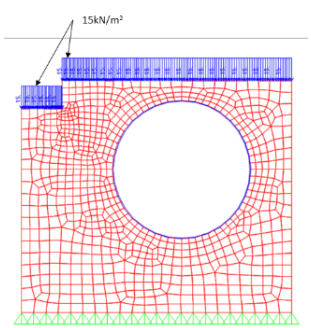

Figure 5.6: Section a-a, SC [kN/m^2] (Fz, global axis).

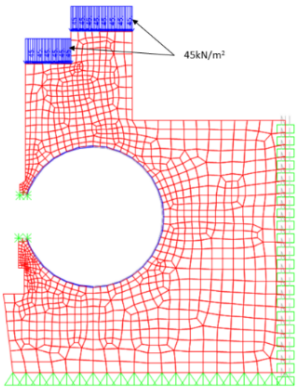

Figure 5.7: Section b-b, RCP [kN/m^2] (Fz, global axis).

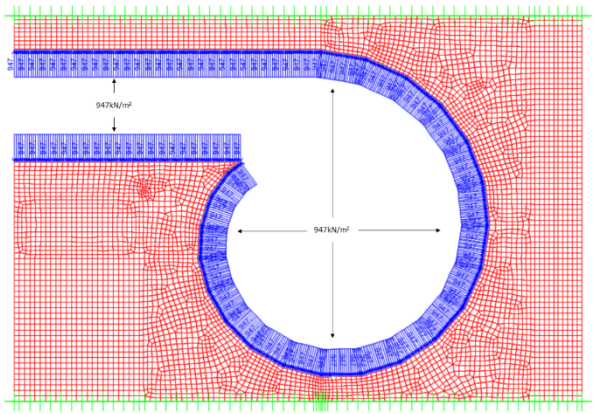

Figure 5.8: Sectionh-h, W [kN/m^2] (F2, local axis).

5.3. Case study 2D FEM results

The following figures present an overall information of the results obtained for ULS for the different sections defined.

Local cross sections were defined to integrate the tension stresses and calculate the corresponding reinforcement.

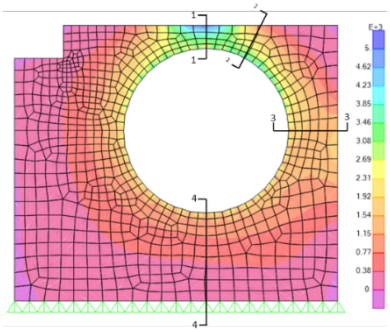

Figure 5.9: Section a-a, Principal tension stress, s_{max}, [kN/m^2]

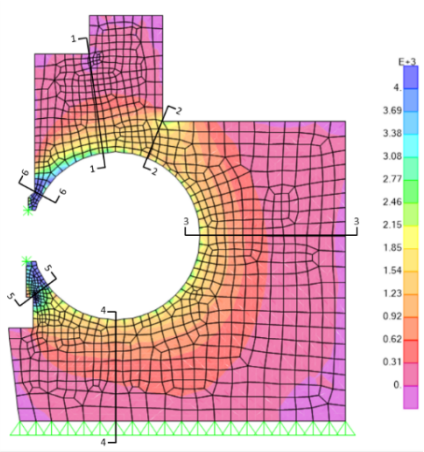

Figure 5.10: Section b-b, Principal tension stress, s_{max}, [kN/m^2]

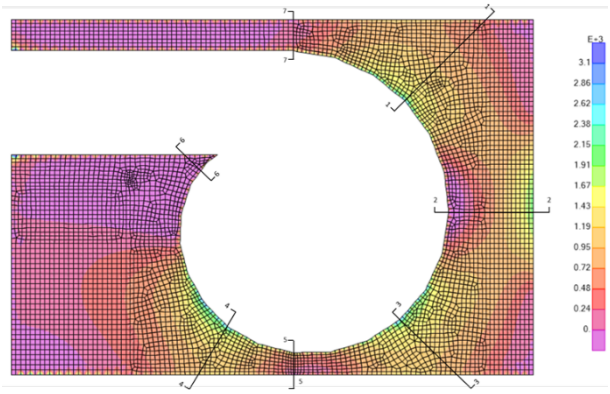

Figure 5.11: Section h-h, Principal tension stress, s_{max}, [kN/m^2]

6. THREE-DIMENSIONAL MODELLING

The use of three-dimensional finite elements modelling enables to analyse in greater detail the extremely complex geometry of the spiral case encasing concrete subjected to the internal pressures.

By this process it is possible to check the interference of the transversal section reduction and better understand how the loads are supported by the principal stresses within the encasing concrete.

This method presents difficulties while modelling the geometry, depending on the FEM software available. For the current work, the software DIANA [13] was the chosen one, as it came up to be the simplest to create automatic 3D solid element mesh.

The 3D solid mesh of the spiral case steel liner (with 30mm thickness) was not included in the model as the priority was to get a not too refined mesh, otherwise convergence issues would rise and calculation time was too long.

For comparison with the previous calculation methods, results were checked for the same cross sections, integrating the stresses the same way to calculate the required reinforcement.

6.1. 3D Model

The FEM software DIANA allows to import the geometry and it automatically creates the solid elements mesh. For this mesh a maximum element edge of 0.50m was defined and the element type brick (20 integration nodes) was chosen as these produce better results than elements type tetrahedron (4 integration nodes).

The following figure presents some views of the mesh produced.

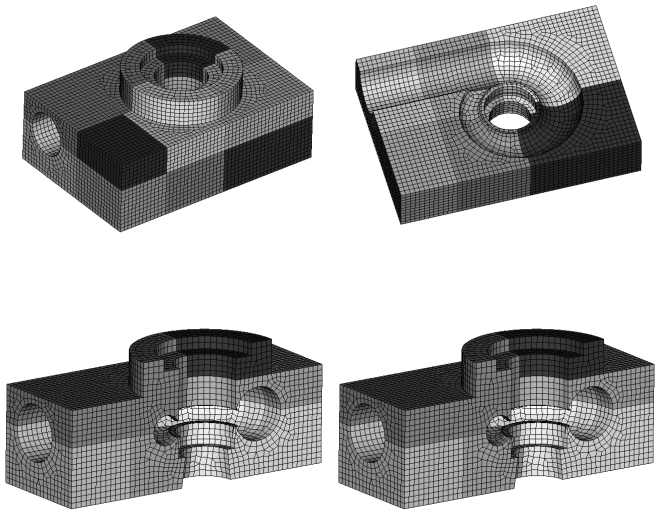

Figure 6.1: FEM mesh, views.

The boundary conditions were set to replicate the restrictions provided by the other parts of the powerhouse structure and adjacent monoliths. Fundamental for the correct distribution of stress was to include the stay ring to close the tension ring provided by the spiral case.

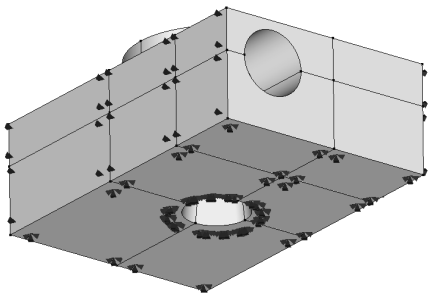

Figure 6.2: FEM, Boundary conditions.

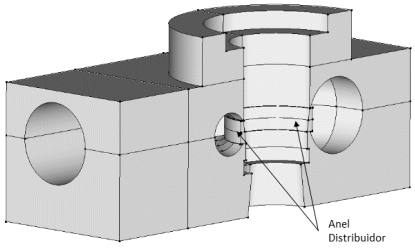

Figure 6.3: FEM, Stay ring.

The previous defined loads were applied, and the following figures show some examples.

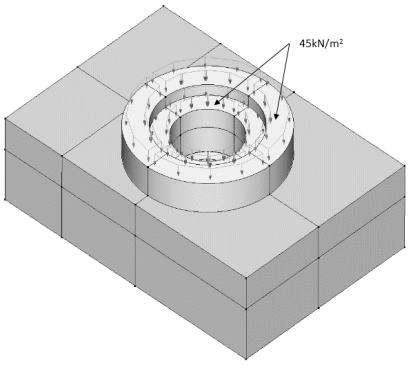

Figure 6.4: Loads, RCP [kN/m^2] (Fz, global axis)

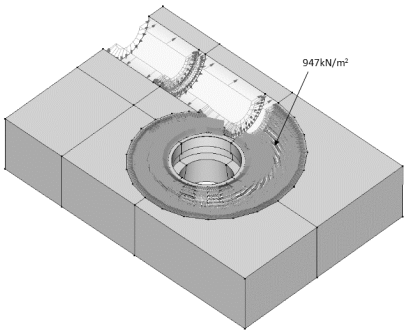

Figure 6.5: Loads, W [kN/m^2]
(local axis orthogonal to surface)

6.2. Results

The following figures present an overall information of the principal tension stress results obtained for ULS. This principal stress is tangent to the spiral case.

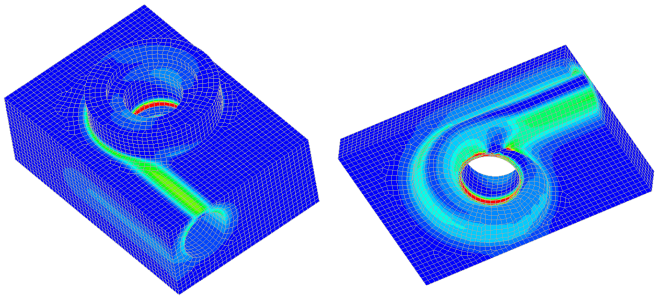

Complete model Top half

Figure 6.6: FEM Results, principal stress S1, ELU [kN/m^2]

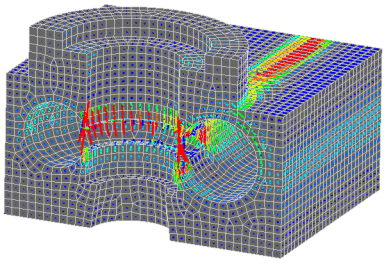

Figure 6.7: FEM Results, principal stress S1, tensors, ELU [kN/m^2]

The following figures present an overall information of the results obtained for ULS for the critical sections previously defined.

Local cross sections were defined to integrate the tension stresses and calculate the corresponding reinforcement.

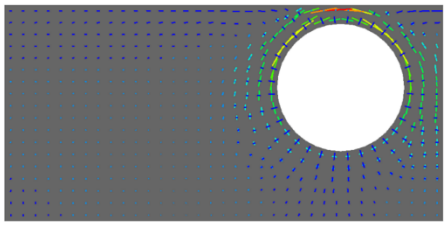

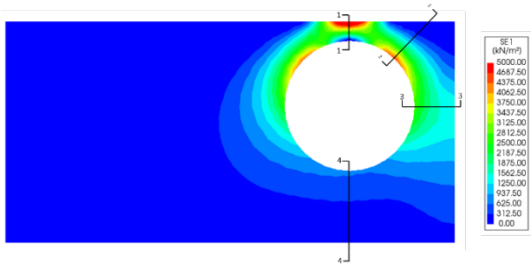

Figure 6.8: Section a-a, Principal tension stress, S1, [kN/m^2]

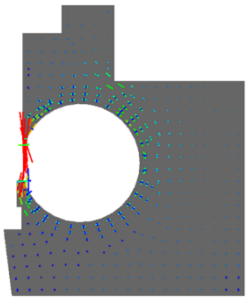

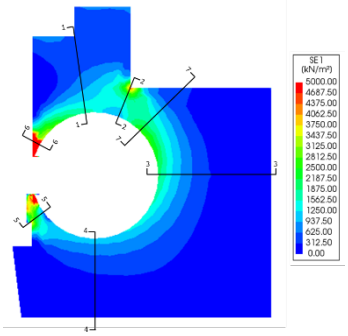

Figure 6.9: Section b-b, Principal tension stress, S1, [kN/m^2]

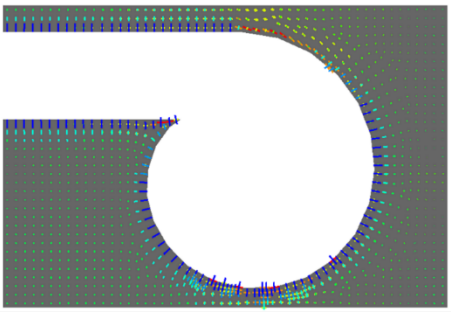

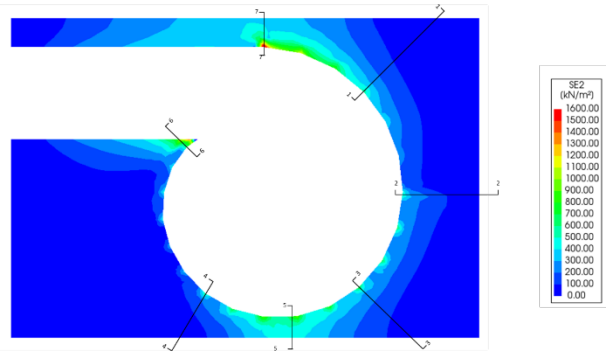

Figure 6.10: Section h-h, Principal tension stress, S2, [kN/m^2]

For additional information the following figure presents the tension principal stress S1, orthogonal to the section h-h plane.

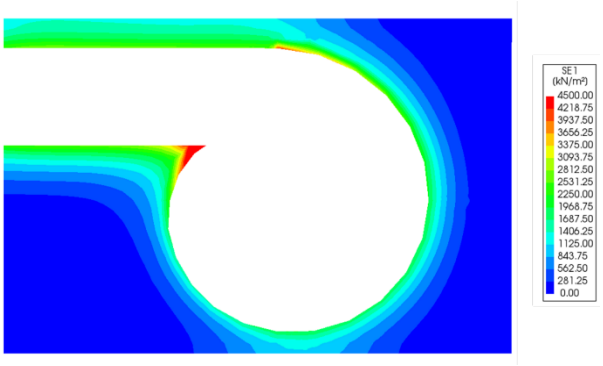

Figure 6.11: Section h-h, Principal tension stress, S1, [kN/m^2] (orthogonal to section plane)

7. COMPARISON ANS ANALYSIS OF THE RESULTS

For the comparison among the 4 different ways used to calculate the spiral case encasing concrete reinforcement (ring reinforcement simplified method, tension ring with Lamé equations simplified method, 2D FEM and 3D FEM), summary of results tables were compiled for each of the critical sections and for the equivalent local integration sections.

7.1. Section a-a

Table 7.1: Summary of results for section a-a

		Seção local 1-1			
		Cálculo Manual		Cálculo FE	
		anel	Lamé	2D	3D
$\sigma_{ct,int}$	[KPa]	0.0	3495.2	2325.0	-280.0
$\sigma_{ct,ext}$	[KPa]	0.0	2645.7	5158.0	6955.0
As_{int}	[cm2/m]	67.7	27.5	24.6	11.6
As_{ext}	[cm2/m]	0.0	23.9	36.6	42.3
As_{total}	[cm2/m]	67.7	51.4	61.3	53.8

		Seção local 2-2			
		Cálculo Manual		Cálculo FE	
		anel	Lamé	2D	3D
$\sigma_{ct,int}$	[KPa]	0.0	3495.2	4055.0	4580.0
$\sigma_{ct,ext}$	[KPa]	0.0	2645.7	970.0	-10.0
As_{int}	[cm2/m]	67.7	27.5	42.4	70.2
As_{ext}	[cm2/m]	0.0	23.9	21.7	10.6
As_{total}	[cm2/m]	67.7	51.4	64.1	80.8

		Seção local 3-3			
		Cálculo Manual		Cálculo FE	
		anel	Lamé	2D	3D
$\sigma_{ct,int}$	[KPa]	0.0	3495.2	1697.0	2750.0
$\sigma_{ct,ext}$	[KPa]	0.0	2645.7	1585.0	1380.0
As_{int}	[cm2/m]	67.7	27.5	28.7	40.7
As_{ext}	[cm2/m]	0.0	23.9	27.7	28.3
As_{total}	[cm2/m]	67.7	51.4	56.4	68.9

		Seção local 4-4			
		Cálculo Manual		Cálculo FE	
		anel	Lamé	2D	3D
$\sigma_{ct,int}$	[KPa]	0.0	3495.2	1301.0	700.0
$\sigma_{ct,ext}$	[KPa]	0.0	2645.7	0.0	-80.0
As_{int}	[cm2/m]	67.7	27.5	28.4	15.8
As_{ext}	[cm2/m]	0.0	23.9	7.4	3.2
As_{total}	[cm2/m]	67.7	51.4	35.8	18.9

Crisscrossing the results from Table 7.1, Figure 5.9, 2D FEM, and Figure 6.8, 3D FEM, it can be concluded that:

- Local integration sections 1-1 and 2-2 results are comparable to a beam fix at both ends subjected to a uniform distributed load, as section 1-1 shows maximum tension stress next to the external face (similar to ½ span) and section 2-2 shows maximum tension stress next to the internal face (similar to fixed support). This results from the fact that the thickness of the encasing concrete increases considerably from section 1-1 to section 2-2, which subsequently provides higher stiffness to section 2-2. Therefore, the results derive considerably from the ones provided by the simplified formulations;
- The results obtained for integration section 3-3 are quite close to the ones foreseen by Lamé equations simplified formulation, although the 3D analysis requires more reinforcement than expected close next to the internal face;
- For integration section 4-4, the results are all quite different, which shows that the boundary restrictions play an important role in the tension stresses closer to the foundation.

7.2. Section b-b

Table 7.2: Summary of results for section b-b

		Seção local 1-1			
		Cálculo Manual		Cálculo FE	
		anel	Lamé	2D	3D
$\sigma_{ct,int}$	[KPa]	0.0	2456.6	3087.0	1800.0
$\sigma_{ct,ext}$	[KPa]	0.0	1543.7	0.0	275.0
As_{int}	[cm2/m]	63.4	29.1	57.3	40.8
As_{ext}	[cm2/m]	0.0	23.0	5.4	15.1
As_{total}	[cm2/m]	63.4	52.1	62.7	55.9

		Seção local 2-2			
		Cálculo Manual		Cálculo FE	
		anel	Lamé	2D	3D
$\sigma_{ct,int}$	[KPa]	0.0	2456.6	1006.0	570.0
$\sigma_{ct,ext}$	[KPa]	0.0	1543.7	2422.0	4350.0
As_{int}	[cm2/m]	63.4	29.1	16.0	14.6
As_{ext}	[cm2/m]	0.0	23.0	25.6	40.1
As_{total}	[cm2/m]	63.4	52.1	41.6	54.7

		Seção local 3-3			
		Cálculo Manual		Cálculo FE	
		anel	Lamé	2D	3D
$\sigma_{ct,int}$	[KPa]	0.0	2456.6	1738.0	2000.0
$\sigma_{ct,ext}$	[KPa]	0.0	1543.7	0.0	-260.0
As_{int}	[cm2/m]	63.4	29.1	48.8	57.6
As_{ext}	[cm2/m]	0.0	23.0	6.2	2.2
As_{total}	[cm2/m]	63.4	52.1	55.0	59.9

		Seção local 4-4			
		Cálculo Manual		Cálculo FE	
		anel	Lamé	2D	3D
$\sigma_{ct,int}$	[KPa]	0.0	2456.6	1411.0	1110.0
$\sigma_{ct,ext}$	[KPa]	0.0	1543.7	87.0	0.0
As_{int}	[cm2/m]	63.4	29.1	31.8	24.2
As_{ext}	[cm2/m]	0.0	23.0	9.0	5.1
As_{total}	[cm2/m]	63.4	52.1	40.8	29.3

		Seção local 5-5			
		Cálculo Manual		Cálculo FE	
		anel	Lamé	2D	3D
$\sigma_{ct,int}$	[KPa]	0.0	2456.6	4836.0	0.0
$\sigma_{ct,ext}$	[KPa]	0.0	1543.7	7252.0	3680.0
As_{int}	[cm2/m]	63.4	29.1	25.3	5.7
As_{ext}	[cm2/m]	0.0	23.0	33.0	17.4
As_{total}	[cm2/m]	63.4	52.1	58.3	23.1

		Seção local 6-6			
		Cálculo Manual		Cálculo FE	
		anel	Lamé	2D	3D
$\sigma_{ct,int}$	[KPa]	0.0	2456.6	4338.0	9500.0
$\sigma_{ct,ext}$	[KPa]	0.0	1543.7	11320.0	7000.0
As_{int}	[cm2/m]	63.4	29.1	14.0	25.2
As_{ext}	[cm2/m]	0.0	23.0	23.3	21.9
As_{total}	[cm2/m]	63.4	52.1	37.2	47.1

		Seção local 7-7			
		Cálculo Manual		Cálculo FE	
		anel	Lamé	2D	3D
$\sigma_{ct,int}$	[KPa]	0.0	2456.6	2993.0	2750.0
$\sigma_{ct,ext}$	[KPa]	0.0	1543.7	-11.0	300.0
As_{int}	[cm2/m]	63.4	29.1	59.6	67.3
As_{ext}	[cm2/m]	0.0	23.0	5.1	22.9
As_{total}	[cm2/m]	63.4	52.1	62.7	90.2

Crisscrossing the results from Table 7.2, Figure 5.10, 2D FEM, and Figure 6.9, 3D FEM, it can be concluded that:

- Local integration sections 1-1, 2-2 and 7-7 results are comparable to a beam fix at both ends subjected to a uniform distributed load, as section 2-2 shows maximum tension stress next to the external face (similar to ½ span) and sections 1-1 and 7-7 show maximum tension stress next to the internal face (similar to fixed support). This results from the fact that the thickness of the encasing concrete increases considerably from section 2-2 to sections 1-1 and 7-7, which subsequently provides higher stiffness to sections 1-1 and 7-7. Therefore, the results derive considerably from the ones provided by the simplified formulations;
- The results obtained for integration section 3-3 are quite close to the ones foreseen by the ring reinforcement simplified formulation, contrarily to section a-a. This shows that for higher

thicknesses Lamé equation formulation doesn't mirror the real behaviour, which is to concentrate the tensions stresses in a ring around the spiral case;

- For integration section 4-4, the results are all quite different, which shows that the boundary restrictions play an important role in the tension stresses closer to the foundation;
- Sections 5-5 and 6-6 clearly show the tension ring around the spiral case.

7.3. Section h-h

Table 7.3: Summary of results for section h-h

		Seção local 1-1			
		Cálculo Manual		Cálculo FE	
		anel	Lamé	2D	3D
$\sigma_{ct,int}$	[KPa]	0.0	2456.6	2900.0	550.0
$\sigma_{ct,ext}$	[KPa]	0.0	1543.7	1070.0	0.0
As_{int}	[cm2/m]	63.4	29.1	125.8	23.4
As_{ext}	[cm2/m]	0.0	23.0	64.7	5.0
As_{total}	[cm2/m]	63.4	52.1	190.5	28.4

		Seção local 2-2			
		Cálculo Manual		Cálculo FE	
		anel	Lamé	2D	3D
$\sigma_{ct,int}$	[KPa]	0.0	2456.6	-625.0	490.0
$\sigma_{ct,ext}$	[KPa]	0.0	1543.7	2044.0	0.0
As_{int}	[cm2/m]	63.4	29.1	-0.4	15.0
As_{ext}	[cm2/m]	0.0	23.0	64.3	3.2
As_{total}	[cm2/m]	63.4	52.1	64.0	18.2

		Seção local 3-3			
		Cálculo Manual		Cálculo FE	
		anel	Lamé	2D	3D
$\sigma_{ct,int}$	[KPa]	0.0	2456.6	3094.0	700.0
$\sigma_{ct,ext}$	[KPa]	0.0	1543.7	1109.0	0.0
As_{int}	[cm2/m]	63.4	29.1	95.8	20.3
As_{ext}	[cm2/m]	0.0	23.0	50.6	4.3
As_{total}	[cm2/m]	63.4	52.1	146.4	24.6

		Seção local 4-4			
		Cálculo Manual		Cálculo FE	
		anel	Lamé	2D	3D
$\sigma_{ct,int}$	[KPa]	0.0	2456.6	3044.0	580.0
$\sigma_{ct,ext}$	[KPa]	0.0	1543.7	1415.0	0.0
As_{int}	[cm2/m]	63.4	29.1	67.5	11.5
As_{ext}	[cm2/m]	0.0	23.0	41.0	2.1
As_{total}	[cm2/m]	63.4	52.1	108.5	13.6

		Seção local 5-5			
		Cálculo Manual		Cálculo FE	
		anel	Lamé	2D	3D
$\sigma_{ct,int}$	[KPa]	0.0	2456.6	2068.0	950.0
$\sigma_{ct,ext}$	[KPa]	0.0	1543.7	-78.0	420.0
As_{int}	[cm2/m]	63.4	29.1	16.1	9.5
As_{ext}	[cm2/m]	0.0	23.0	1.8	5.9
As_{total}	[cm2/m]	63.4	52.1	17.8	15.4

		Seção local 6-6			
		Cálculo Manual		Cálculo FE	
		anel	Lamé	2D	3D
$\sigma_{ct,int}$	[KPa]	0.0	2456.6	-1402.0	1450.0
$\sigma_{ct,ext}$	[KPa]	0.0	1543.7	-818.0	920.0
As_{int}	[cm2/m]	63.4	29.1	0.0	24.9
As_{ext}	[cm2/m]	0.0	23.0	0.0	19.6
As_{total}	[cm2/m]	63.4	52.1	0.0	44.5

		Seção local 7-7			
		Cálculo Manual		Cálculo FE	
		anel	Lamé	2D	3D
$\sigma_{ct,int}$	[KPa]	0.0	2456.6	1680.0	1870.0
$\sigma_{ct,ext}$	[KPa]	0.0	1543.7	1012.0	340.0
As_{int}	[cm2/m]	63.4	29.1	17.1	21.6
As_{ext}	[cm2/m]	0.0	23.0	11.1	7.7
As_{total}	[cm2/m]	63.4	52.1	190.5	29.3

Crisscrossing the results from Table 7.3, Figure 5.11, 2D FEM, and Figure 6.10 and Figure 6.11, 3D FEM, it can be concluded that:

- The results from the 3D FEM are significantly smaller to the ones obtained by the other calculation methods, but are considered to the the correct ones because:
  - Either simplified formulations and 2D FEM, assume as a starting point that the internal load is fully supported in the plane of analysis, which is, for section h-h, the horizontal plane through the axis of the spiral case. Well this is far from reality, as already mentioned in 5.1 (ring reinforcement formulation) the main "span" is the transversal, behaving the spiral case shell as a one-way slab. Therefore, the resulting stresses are over dimensioned;
  - Two-dimensional models only consider the geometry of the section at the spiral case axis, conceptualizing the analysis as problem as a slice of 1m of an infinite "cylinder". This is completely far from the reality, due to the circular shape of the transversal section, stiffness immediately increases as the horizontal plane gets further away from the spiral case axis. Associating this with the fact that the direction of the internal pressure is always orthogonal to the surface, it results that the tension stresses rapidly decrease as soon as the encasing concrete thickness increases as we move away from the minimum values located precisely at the spiral case axis. . Evento bem visível na Figure 6.6Figure 6.6: FEM .

8. VERIFICATION OF LIMIT STATES AND REINFORCEMENT DESIGN AND DETAILING

In order to take in consideration the SLS previously mentioned in 3.3, the reinforcement yield strength was limited to:

$$f_{yd,SLS} = \frac{f_{yd}}{H_f} = \frac{435}{1,65} = 263MPa$$

As spiral case encasing concrete is a mass concrete, minimum reinforcement was defined according to ACI350 [14] table 7.12.12.1.

Following the conclusions presented in 7, the final design of the reinforcement required used the results from the 3D FEM.

As an example, design for section b-b is presented in Table 8.1and reinforcement sketch presented in Figure 8.1.

Table 8.1: Section b-b, reinforcement design for SLS.

Secção		**1-1**	**2-2**	**3-3**	**4-4**	**5-5**	**6-6**	**7-7**
$A_{s,cir,int,calc}$	[cm²/m]	67,5	24,2	95,3	40,0	15,3 (*)	41,7	111,3
$A_{s,cir,int,adopt}$		Ø32//0.20 (1ª camada) + Ø32//0.20 (2ª camada)	Ø32//0.20 (1ª camada) + Ø32//0.20 (2ª camada)	Ø32//0.20 (1ª camada) + Ø32//0.20 (2ª camada) + Ø32//0.20 (3ª camada)	Ø32//0.20	Ø32//0.20	Ø32//0.20 (1ª camada) + Ø32//0.20 (2ª camada)	Ø32//0.20 (1ª camada) + Ø32//0.20 (2ª camada) + Ø32//0.20 (3ª camada)
	[cm²/m]	80,4	80,4	120,6	40,2	40,2	80,4	120,6
$A_{s,cir,ext,calc}$	[cm²/m]	25,0	66,3	15,3 (*)	15,3 (*)	28,7	36,2	37,8
$A_{s,cir,ext,adopt}$		Ø32//0.20	Ø32//0.20 (1ª camada) + Ø32//0.20 (2ª camada)	Ø20//0.20	Ø20//0.20	Ø25//0.20+ Ø20//0.20 (1ª camada)	Ø25//0.20 (1ª camada) + Ø20//0.20 (2ª camada)	Ø32//0.20 (1ª camada) + Ø32//0.20 (2ª camada)
	[cm²/m]	40,2	80,4	15,7	15,7	40,2	40,3	80,4

(*) - $A_{s,min}$

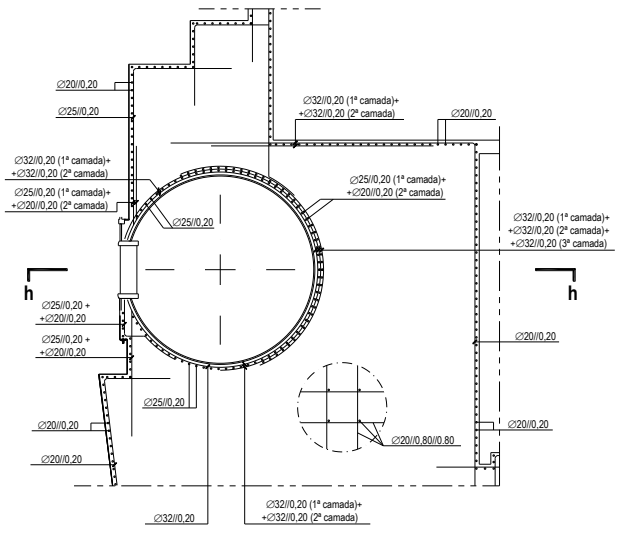

Figure 8.1: Section b-b, reinforcement sketch.

9. FINAL CONSIDERATIONS

The structural design of the spiral case encasing concrete is a highly complex task that requires special care in the way to determine and analyse the configuration of the tension stresses in the mass concrete.

Due to the intricate geometry, it was concluded that the direct application of simplified analysis might not correspond to the reality. Therefore, it should be further investigated in a more detailed level how the internal spiral case loads are shared between the steel liner and the encasing concrete.

Over all, it was confirmed that the use of simplified methods provides tools to calibrate the more complex calculation models. It was confirmed that, for this type of structures, three-dimensional modelling with solid finite elements is the most complete way to guarantee that no zone of stresses convergence is left unchecked.

Nevertheless, it way possible to see that the choice of FEM software for three-dimensional calculation is crucial to have or not success in modelling in a expedite way the geometry, generate automatic finite elements meshes and visualise/analyse the results. It must be noticed that the refinement of the mesh is equally important, because if it is too fine there is the risk that it requires too much computation capacity, but if it is too big it might not follow closely the changes in the geometry.

Also important is to correctly consider the boundary conditions in the FEM, as the results will vary considerably, namely the presence of the stay ring connecting the two ends of the spiral case and the horizontal compression restriction provided by the adjacent monoliths.

To be developed in future studies is to add to the three-dimensional model the steel liner in order to check the share of stresses between the spiral case and the encasing concrete, which will allow to reduce the required reinforcement.

10. REFERENCES

[1] ASCE (1989), *Civil Engineering Guidelines for Planning and Designing Hydroelectric Developments, Volume 3: Powerhouses and Related Topics*, New York;

[2] de Souza, Z, H. M. Santos, A, da C. Bortoni, E (1999), *Centrais Hidrelétricas, Estudos para Implantação*, Centrais Eléctricas Brasileiras S.A. – Eletrobrás;

[3] C. S. Lamego, M. (2014), *Dimensionamento Estrutural de uma Central Hidroeléctrica a Céu Aberto*, Tese de dissertação, Instituto Superior Técnico;

[4] Nigam P.S (1985), *Handbook of Hydro Electric Engineering*, Nem Chand and Brothers, Roorkee;

[5] Camelo, A. (2011), *Durabilidade e Vida Útil das Estruturas Hidráulicas de Betão e de Betão Armado*, 1as Jornadas de Materiais na Construção;

[6] NP EN 1990:2009 – *Bases para o Projeto de estruturas*;

[7] NP EN 1992-1-1:2010 – *Projeto de estruturas de betão, Parte 1-1: Regras gerais e regras para edifícios*;

[8] SIA 260:2003 – *Basis of structural design*;

[9] SIA 262:2003 – *Concrete Structures*;

[10] Sítio da internet http://mechanicstips.blogspot.com/2016/08/spiral-case-of-water-turbine.html consultado a 6 de março de 2019;

[11] Carlos Oliveira, Verónica Gama, Rui Vaz Rodrigues and Acácio Santo (2012). Central do Reforço de Potência do Escalão de Alqueva. Encontro Nacional de Betão Estrutural 2012;

[12] USACE EM 1110-2-2104 - Strength Design for Reinforced Concrete Hydraulic Structures, DEPARTMENT OF THE ARMY, U.S. Army Corps of Engineers, Washington, DC;

[13] DIANA – Finite Element Analysis, DIANA Documentation release 10.3, *First edition, March 1, 2019.* DIANA FEA bv;

[14] ACI 350-01 – Code requirements for environmental engineering concrete structures.